Transition from amplitude to oscillation death under mean-field diffusive coupling

Tanmoy Banerjee* and Debarati Ghosh
Department of Physics, University of Burdwan, Burdwan 713 104, West Bengal, India
(Received 12 March 2014; published 23 May 2014)

We study the transition from the amplitude death (AD) to the oscillation death (OD) state in limit-cycle oscillators coupled through mean-field diffusion. We show that this coupling scheme can induce an important transition from AD to OD even in identical limit cycle oscillators. We identify a parameter region where OD and a nontrivial AD (NTAD) state coexist. This NTAD state is unique in comparison with AD owing to the fact that it is created by a subcritical pitchfork bifurcation and parameter mismatch does not support this state, but destroys it. We extend our study to a network of mean-field coupled oscillators to show that the transition scenario is preserved and the oscillators form a two-cluster state.

DOI: 10.1103/PhysRevE.89.052912 PACS number(s): 05.45.Xt

I. INTRODUCTION

Oscillation quenching is an emergent and intriguing phenomenon that has been the topic of extensive research in diverse fields such as physics, biology, and engineering [1]. There are two distinct types of oscillation quenching processes: amplitude death (AD) and oscillation death (OD). In AD coupled oscillators arrive at a common stable steady state that was unstable otherwise and thus form a stable homogeneous steady state (HSS) [2,3]. However, in the case of OD, oscillators populate different coupling-dependent steady states and thus give rise to stable inhomogeneous steady states (IHSSs); in the phase space OD may coexist with limit cycle oscillations. Amplitude death is important in the case of control applications where suppression of unwanted oscillations is necessary, e.g., in laser application [4] and neuronal systems [5]. On the other hand, OD is a much more complex phenomenon because it induces inhomogeneity in a rather homogeneous system of oscillators that has strong connections and importance in the field of biology (e.g., a synthetic genetic oscillator [6] and cellular differentiation [7]), physics [8], etc.

Although AD and OD are two structurally different phenomena (their genesis and manifestations are different), for many years they were (erroneously) treated on the same footing. Only recently have pioneering works in Refs. [1,9,10] established the much needed distinctions between AD and OD (see Ref. [1] for an extensive review on OD). Although extensive research has been reported on AD (see [2] and references therein), the phenomenon of OD is a less explored topic. Koseska *et al.* [9] show that AD and OD can simultaneously occur in diffusively coupled Stuart-Landau oscillators; they show also an important transition phenomenon, namely, the transition from AD to OD in Stuart-Landau oscillators with parameter mismatch. Their work established that the transition occurs due to the interplay between the heterogeneity and the coupling parameter that is analogous to the Turing-type bifurcation [11] in spatially extended systems. In [10] it was shown that the presence of time delay enhances the effect of the AD-OD transition as well as that the AD-OD transition can be induced even in the identical Stuart-Landau oscillators by using dynamic [12] and conjugate [13] coupling. Reference [14] shows the transition between AD and OD in identical nonlinear oscillators that are coupled diffusively and perturbed by a symmetry-breaking repulsive coupling link.

In the above-mentioned studies the role of mean-field diffusive coupling in the occurrence of OD and the AD-OD transition are not considered; mean-field coupling is one of the most widely studied topics because of its presence in many natural phenomena in the fields of biology, physics, and engineering [15–18]. All of the previous studies show that the mean-field coupling in oscillators can induce AD only [15–17]. Only in Refs. [19,20], in the context of genetic oscillators interacting through a quorum-sensing mechanism, the occurrence of OD is shown where the concentration of the autoinducer molecule that can diffuse through the cell membrane contains a mean-field term, but no AD-OD transition is reported there. In this paper we systematically explore that the mean-field coupling can induce a Turing-type transition from AD (stable HSS) to OD (stable IHSS) even in identical limit cycle oscillators. Further, we identify an important parameter regime where OD coexists with a different nontrivial AD (NTAD) state. This NTAD state is unique in comparison with its conventional counterpart in at least two ways. First, unlike AD, which has two possible routes, i.e., Hopf and saddle-node bifurcation, the NTAD state is born via a subcritical pitchfork bifurcation. Second, in sharp contrast to the AD, which is supported or enhanced by parameter mismatch, the NTAD state is completely destroyed by parameter mismatch. In this paper we consider a single paradigmatic oscillator, namely, the Stuart-Landau oscillator, which is widely used in the literature on the studies of OD and AD and their transitions [1,9,10]. We also extend our study to a network of oscillators and show that the occurrence of OD and the AD-OD transition are preserved for more than two oscillators.

II. STUART-LANDAU OSCILLATORS WITH MEAN-FIELD COUPLING

We consider a number N of Stuart-Landau oscillators interacting through mean-field diffusive coupling; a mathematical model of the coupled system is given by

$$\dot{Z}_i = (1 + i\omega_i - |Z_i|^2)Z_i + \epsilon[Q\overline{Z} - \text{Re}(Z_i)], \qquad (1)$$

*tbanerjee@phys.buruniv.ac.in

with $i = 1, \ldots, N$; $\overline{Z} = \frac{1}{N}\sum_{i=1}^{N} \mathrm{Re}(Z_i)$ is the mean field of the coupled system $Z_i = x_i + jy_i$. The individual Stuart-Landau oscillators are of unit amplitude and having eigenfrequency ω_i. The coupling strength is given by ϵ and Q is a control parameter that determines the density of the mean field [16,17,20] ($0 \leq Q \leq 1$); $Q \to 0$ indicates the self-feedback case, whereas $Q \to 1$ represents the maximum mean-field density. As the limiting case we take $N = 2$ and write (1) in Cartesian coordinates

$$\dot{x}_{1,2} = P_{1,2}x_{1,2} - \omega_{1,2}y_{1,2} + \epsilon[Q\overline{X} - x_{1,2}], \tag{2a}$$

$$\dot{y}_{1,2} = \omega_{1,2}x_{1,2} + P_{1,2}y_{1,2}. \tag{2b}$$

Here $P_i = 1 - x_i^2 - y_i^2$ $(i = 1,2)$ and $\overline{X} = \frac{x_1+x_2}{2}$. At first we consider the case of two identical oscillators, i.e., $\omega_{1,2} = \omega$. From Eq. (2) it is clear that the system has the trivial fixed point, which is the origin (0,0,0,0), and additionally two coupling-dependent nontrivial fixed points $(x_1^*, y_1^*, -x_1^*, -y_1^*)$, where $x_1{}^* = -\frac{\omega y_1^*}{\omega^2+\epsilon y_1^{*2}}$ and

$$y_1{}^* = \sqrt{\frac{(\epsilon - 2\omega^2) + \sqrt{\epsilon^2 - 4\omega^2}}{2\epsilon}},$$

and $(x_1^\dagger, y_1^\dagger, x_1^\dagger, y_1^\dagger)$, where

$$x_1^\dagger = -\frac{\omega y_1^\dagger}{\epsilon(1-Q)y_1^{\dagger 2} + \omega^2}$$

and

$$y_1^\dagger = \sqrt{\frac{\epsilon(1-Q) - 2\omega^2 + \sqrt{(\epsilon - \epsilon Q)^2 - 4\omega^2}}{2\epsilon(1-Q)}}.$$

Note that the existence of these nontrivial fixed points was not explored in the earlier study of mean-field coupled Stuart-Landau oscillators [16]. In the following sections we will examine different dynamical regions and their transitions based on the eigenvalue analysis; subsequently, we carry out bifurcation analysis using the package XPPAUT [21].

III. THE AD-OD TRANSITION AND EMERGENCE OF NONTRIVIAL AD

The four eigenvalues of the system at the trivial fixed point (0,0,0,0) are

$$\lambda_{1,2} = 1 - \left[\frac{\epsilon(1-Q) \pm \sqrt{\epsilon^2(1-Q)^2 - 4\omega^2}}{2}\right], \tag{3a}$$

$$\lambda_{3,4} = 1 - \left[\frac{\epsilon \pm \sqrt{\epsilon^2 - 4\omega^2}}{2}\right]. \tag{3b}$$

Eigenvalue analysis and also a close inspection of the nontrivial fixed points reveal that the system has two pitchfork bifurcations given by PB1 and PB2 occurring at the following values of the coupling parameters, respectively:

$$\epsilon_{\mathrm{PB1}} = 1 + \omega^2, \tag{4a}$$

$$\epsilon_{\mathrm{PB2}} = \frac{1+\omega^2}{1-Q}. \tag{4b}$$

Here ϵ_{PB1} is that value where a symmetry breaking pitchfork bifurcation gives birth to the nontrivial fixed point $(x_1^*, y_1^*, -x_1^*, -y_1^*)$, i.e., the IHSS emerges at this value of coupling parameter. It is noteworthy that the occurrence of PB1 does not depend upon the density parameter Q (but later we will see that stability of the IHSS depends on Q). The second nontrivial fixed point $(x_1^\dagger, y_1^\dagger, x_1^\dagger, y_1^\dagger)$ arises at PB2; PB2 gives rise to a unique nontrivial HSS. Later we will see that stabilization of this state leads to a different NTAD state that coexists with OD.

Next we search for the Hopf bifurcation point at which the stable oscillation dies to give birth to the AD state. From (3) it is clear that for $\omega \leqslant 1$ no Hopf bifurcations (of trivial fixed point) occur; only pitchfork bifurcations govern the dynamics in that case. For any $\omega > 1$, equating the real part of $\lambda_{3,4}$ and $\lambda_{1,2}$ to zero we get

$$\epsilon_{\mathrm{HB1}} = 2, \tag{5a}$$

$$\epsilon_{\mathrm{HB2}} = \frac{2}{1-Q}, \tag{5b}$$

respectively; here ϵ_{HB1} and ϵ_{HB2} are the values of coupling parameters where the first (HB1) and the second (HB2) Hopf bifurcation occur, respectively. From (5) it is clear that ϵ_{HB1} is constant, but ϵ_{HB2} depends only upon the value of Q (and independent of ω, where $\omega > 1$). Now, when $Q \to 0$, $\epsilon_{\mathrm{HB1}} \approx \epsilon_{\mathrm{HB2}}$. Figure 1(a) shows the bifurcation diagram of $x_{1,2}$ for $Q = 0.3$ and $\omega = 2$ (without any loss of generality, unless stated otherwise, we take $\omega = 2$). It is observed that at HB2 an inverse Hopf bifurcation occurs and the stable limit cycle is suppressed to give birth to AD (i.e., a stable HSS), whereas at HB1 an unstable limit cycle is born. This stable HSS (AD) becomes unstable through a supercritical pitchfork bifurcation (PB1) at $\epsilon_{\mathrm{PB_1}} = 1 + \omega^2 = 5$. Here the trivial fixed point becomes unstable and two new stable IHSSs are created, giving birth to OD. Thus, we get a transition between AD and OD in identical mean-field coupled oscillators. With a further increase in coupling strength ϵ, PB2 occurs at $\epsilon_{\mathrm{PB2}} = 7.142$ [which agrees with (4b)], which gives birth to a nontrivial HSS (i.e., $x_1^\dagger = x_2^\dagger$). This nontrivial HSS is stabilized via subcritical pitchfork bifurcation (PBS) at $\epsilon_{\mathrm{PBS}} \approx 8.05$ and gives rise to a different NTAD state. We attach the attribute nontrivial to this AD state because it emerges from the nontrivial HSSs $(x^\dagger, y^\dagger)$, which are nonzero and subsequently placed symmetrically around zero. We also verify the occurrence of this pitchfork bifurcation directly from the eigenvalues corresponding to $(x_1^\dagger, y_1^\dagger, x_1^\dagger, y_1^\dagger)$, which are given by

$$\lambda_{1,2}^\dagger = 1 - \frac{b_1^\dagger}{2} \pm \frac{\sqrt{b_1^{\dagger 2} - 4c_1^\dagger}}{2}, \tag{6a}$$

$$\lambda_{3,4}^\dagger = 1 - \frac{b_2^\dagger}{2} \pm \frac{\sqrt{b_2^{\dagger 2} - 4c_2^\dagger}}{2}, \tag{6b}$$

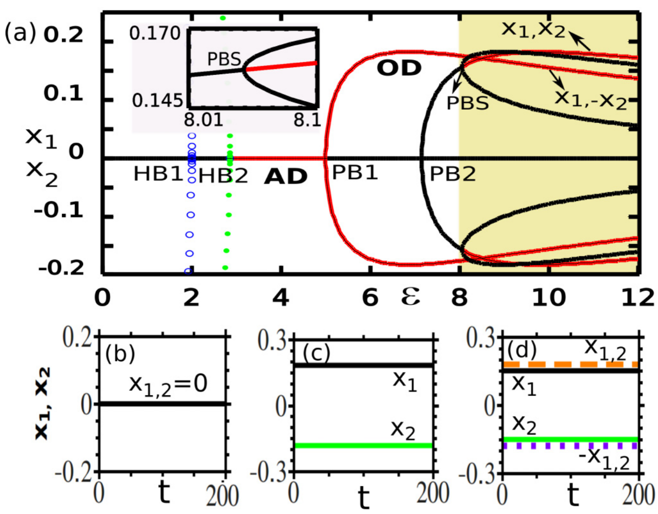

FIG. 1. (Color online) (a) Bifurcation diagram (using XPPAUT) of two mean-field coupled identical Stuart-Landau oscillators ($Q = 0.3$, $\omega = 2$): gray (red) lines, stable fixed points; black lines, unstable fixed points; closed (green) circles, stable limit cycle; and open (blue) circles, unstable limit cycle. HB1,2 and PB1,2 are Hopf and pitchfork bifurcation points, respectively. PBS denotes the subcritical pitchfork bifurcation point; the inset shows the zoomed-in view of the region of occurrence of PBS. AD is created at HB2 and PB1 gives the AD-OD transition point. The coexistence of OD ($x_1 = -x_2$) and NTAD ($x_1 = x_2$) is shown in the shaded (yellow) region. Time traces are shown for (b) AD ($x_{1,2} = 0$) at $\epsilon = 4$, (c) OD ($x_1 = -x_2$) at $\epsilon = 7$, and (d) NTAD and OD at $\epsilon = 10.92$; here dashed and dotted lines represent two initial condition-dependent NTAD states $x_{1,2}$ and $-x_{1,2}$, respectively.

where $b_1^\dagger = (\epsilon - \epsilon Q + 4x_1^{\dagger 2} + 4y_1^{\dagger 2})$, $c_1^\dagger = (x_1^{\dagger 2} + 3y_1^{\dagger 2})(\epsilon - \epsilon Q + 3x_1^{\dagger 2} + y_1^{\dagger 2}) + \omega^2 - 4x_1^{\dagger 2} y_1^{\dagger 2}$, $b_2^\dagger = (\epsilon + 4x_1^{\dagger 2} + 4y_1^{\dagger 2})$, and $c_2^\dagger = (x_1^{\dagger 2} + 3y_1^{\dagger 2})(\epsilon + 3x_1^{\dagger 2} + y_1^{\dagger 2}) + \omega^2 - 4x_1^{\dagger 2} y_1^{\dagger 2}$. Since stable IHSS (OD) solutions [corresponding to the first nontrivial fixed points (x^*, y^*)] still exist beyond this coupling value OD and NTAD coexist for $\epsilon \geqslant \epsilon_{\rm PBS}$ [shaded (yellow) region in Fig. 1(a)]. The coexistence of OD and another kind of nontrivial AD was found earlier in conjugate coupled Stuart-Landau oscillators in [10], but here the genesis of NTAD and the origin of coexistence is different from that; in our case subcritical pitchfork bifurcation is responsible for the NTAD state. Further, in the NTAD state we have two different solutions $x_1 = x_2$ and $-x_1 = -x_2$; the occurrence of one of these two states is determined by the initial conditions. This has a striking resemblance to bistability, but here the bistability is much more subtle owing to the fact that, unlike its classical counterpart, it coexists with OD and it emerges via a subcritical pitchfork bifurcation. Later we will see that any parameter mismatch destroys this NTAD state. This initial condition-dependent amplitude death state was not observed earlier. To confirm the coexistence of OD and NTAD we integrate the system equation with suitably chosen initial conditions (using the fourth-order Runge-Kutta method, with step size equal to 0.005); Fig. 1(d) shows this for $\epsilon = 10.92$, where we can see that the OD state and NTAD states coexist.

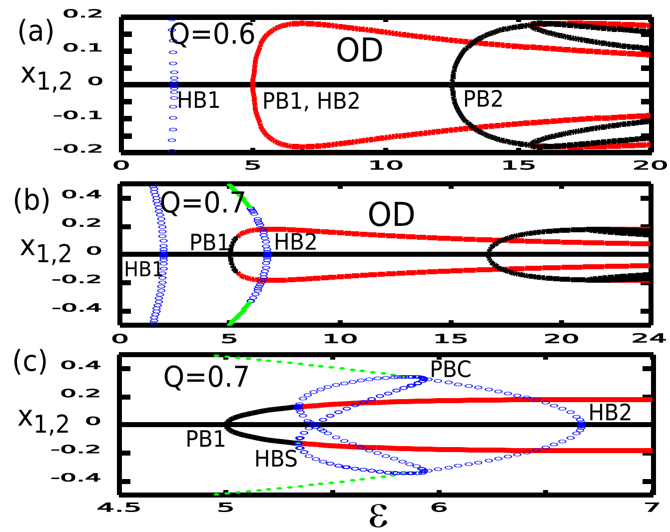

FIG. 2. (Color online) The AD state vanishes when HB2 is equal to PB1 at (a) $Q = Q^*$ ($= 0.6$) and (b) and (c) $Q > Q^*$ ($= 0.7$): HB2 moves to the right side of PB1 and the nontrivial fixed point gains stability by subcritical Hopf bifurcation (HBS). Between HBS and pitchfork bifurcation of the limit cycle, the coexistence of a stable limit cycle, an unstable limit cycle, and OD is observed. The other parameter is $\omega = 2$.

Figures 1(b) and 1(c) show the AD ($\epsilon = 4$) and OD ($\epsilon = 7$) states, respectively.

Now, with an increasing Q value, $\epsilon_{\rm HB2}$ will move towards $\epsilon_{\rm PB1}$ and the zone of stable HSS (AD) decreases. For a given ω (where $\omega > 1$) at a particular Q value (say, Q^*), $\epsilon_{\rm HB2}$ will collide with $\epsilon_{\rm PB1}$. So at $Q = Q^*$, $\epsilon_{\rm HB2} = \epsilon_{\rm PB1}$, i.e., $Q^* = \frac{\omega^2 - 1}{\omega^2 + 1}$. At this point, the ϵ region where AD occurs vanishes and thus the AD to OD transition does not occur. Figure 2(a) shows this scenario for $\omega = 2$ and $Q = 0.6$. Now, for $Q > Q^*$, $\epsilon_{\rm HB2} > \epsilon_{\rm PB1}$, i.e., the HB2 point moves towards the right-hand side of PB1; subsequently, the IHSS now gains stability at $\epsilon_{\rm HBS}$ through a subcritical Hopf bifurcation; in Figs. 2(b) and 2(c) for $Q = 0.7$ we get $\epsilon_{\rm HBS} \approx 5.341$. This can be predicted from the eigenvalues of the nontrivial fixed point $(x_1^*, y_1^*, -x_1^*, -y_1^*)$, which are the same as in (6) but with the daggers replaced by asterisks. From the eigenvalue equations we find $\epsilon_{\rm HBS}$, where the IHSS regains stability:

$$\epsilon_{\rm HBS} = \frac{-2(Q+1) + 4\sqrt{1 + \omega^2 (1-Q)(3+Q)}}{(1-Q)(3+Q)}. \qquad (7)$$

The value of $\epsilon_{\rm HBS}$ agrees with Figs. 2(b) and 2(c). The HB2 point gives birth to an unstable limit cycle that becomes stable through a pitchfork bifurcation of the limit cycle (PBC). Between HBS and PBC, stable and unstable limit cycles coexist with OD. In this region we identify (not shown here) three distinct dynamical behaviors: a homogeneous limit cycle, an inhomogeneous limit cycle, and OD. We capture the whole bifurcation scenario in the Q-ϵ parameter space (Fig. 3). We can see that, with increasing Q, at $Q = 0.6$, HB2 collides with PB1, thus destroying the AD-OD transition. Also shown is the coexisting region of NTAD and OD that is determined by the PBS curve. In the previous studies on the mean-field coupled Stuart-Landau oscillators only the transition from

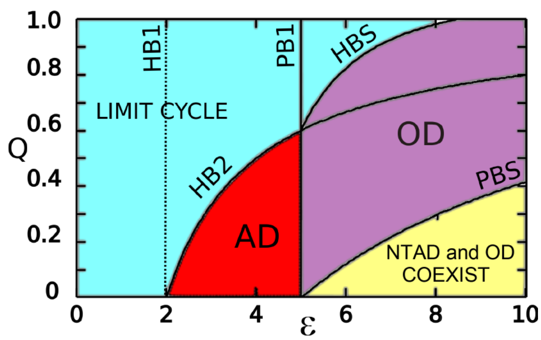

FIG. 3. (Color online) Phase diagram in Q-ϵ space ($\omega = 2$). With increasing Q, the collision of HB2 and PB1 destroys the AD-OD transition scenario.

the limit cycle to AD was shown [16]; here we identify additional bifurcation scenarios and dynamical regions. Before we proceed further let us summarize our results of the AD-OD transition: (i) For $Q < Q^*$ and $\epsilon_{HB2} < \epsilon_{PB1}$, the AD-OD transition occurs. (ii) For $Q = Q^*$ and $\epsilon_{HB2} = \epsilon_{PB1}$, there is no AD, only a stable IHSS (OD), and the AD-OD transition vanishes. (iii) For $Q > Q^*$ and $\epsilon_{HB2} > \epsilon_{PB1}$, the IHSS gains stability at ϵ_{HBS} and the OD moves to the right-hand side with increasing Q.

IV. PARAMETER MISMATCH AND CLUSTER FORMATION

We examine the effect of parameter mismatch on the coupled dynamics. We introduce a mismatch parameter Δ in Eq. (2) defined by $\Delta = \omega_2/\omega_1$. Here $\Delta = 1$ represents the case of no mismatch. For $\Delta \neq 1$, nontrivial fixed points of (2) cannot be derived in a closed form, thus we use XPPAUT to locate them and subsequently test their stability. To get a detailed scenario of the dynamical behaviors we compute the two-parameter bifurcation diagram in Δ-ϵ space for a given Q and ω_1. Figure 4(a) shows this for $Q = 0.3$ and $\omega_1 = 2$. It can be observed that for the mismatched case AD occurs at a lower value of ϵ. It is noteworthy that the HB2 curve is symmetrical around the $\Delta = 1$ line; this is expected as HB2 does not depend upon ω (as long as $\omega > 1$). The OD is governed by the PB1 curve, which depends upon the frequency of oscillators and thus on the value of Δ. For $\Delta < 1$, PB1 comes closer to HB2, thus reducing the zone of AD and broadening the zone of OD. At $\Delta \approx 0.54$, PB1 and HB2 collide to eliminate the zone of AD and thus destroy the AD-OD transition. For $\Delta > 1$, PB1 moves far from HB2, enhancing the zone of AD and also supporting the AD-OD transition. Thus, we see that besides Q, the AD-OD transition is determined by the parameter mismatch also. We have made another important observation in the mismatched case: The nontrivial HSS created at PB2 does not become stable for any $\Delta \neq 1$. Thus, for the parameter mismatched case no NTAD state occurs. As an illustrative example, Fig. 4(b) shows that no NTAD occurs, making OD the only possible solution beyond PB1 ($\Delta = 1.1$, $Q = 0.3$, and $\omega_1 = 2$). Nevertheless, the nontrivial HSS (although unstable) still exists, even in the parameter mismatched case.

Next we investigate the more general case of $N > 2$. At first let us take $N = 3$ and $\Delta = 1$; now the coupled equation is

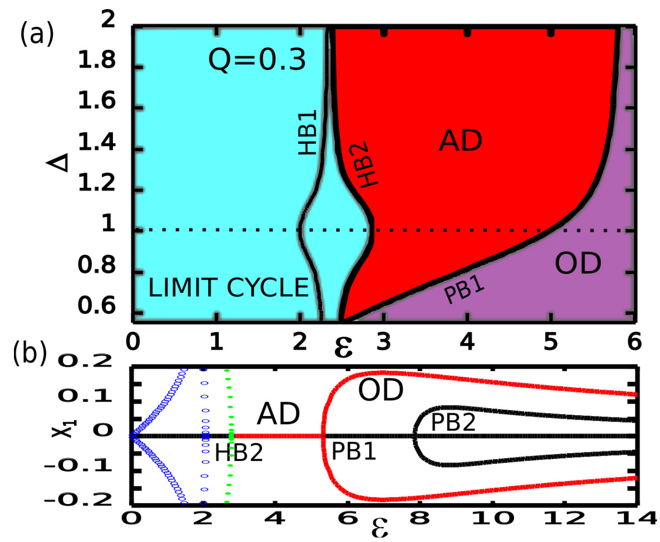

FIG. 4. (Color online) (a) Phase diagram in Δ-ϵ space for $Q = 0.3$ and $\omega_1 = 2$. The NTAD state vanishes for any $\Delta \neq 1$; this is shown in (b) for $\Delta = 1.1$.

given by Eq. (1) with $i = 1,2,3$. Besides the trivial fixed point, there exist other nontrivial solutions with combinations such as (α,α,α), (α,β,α), and (α,α,β) and their cyclic permutations [10]. The (α,α,α) set gives the nontrivial HSS and the remaining sets give IHSS solutions. Figure 5(a) shows this scenario for $\omega = 2$ and $Q = 0.5$. Here also we can observe the occurrence of the AD-OD transition and the coexistence of OD and NTAD. Next we consider the network of $N = 256$ mean-field coupled oscillators; Fig. 5(b) shows the space-time plot of stable IHSS (OD) solutions for $\Delta = 1$, $\epsilon = 16$, $\omega = 3$, and $Q = 0.5$ (for clarity the first 150 elements are shown). The figure clearly shows the formation of a two-cluster solution. Further, we observe that (not shown here) in the space-time plot the size and position of the domains change with the number of elements N and initial conditions; clearly this fact has a

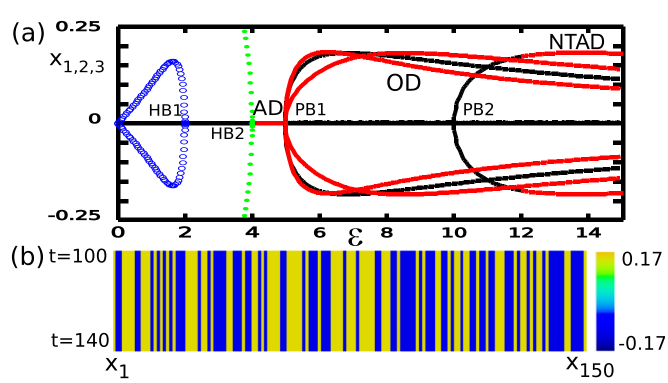

FIG. 5. (Color online) (a) Bifurcation for $N = 3$ ($\omega = 2$): The AD-OD transition is preserved and the NTAD state (α,α,α) coexists with OD. (b) Two-cluster pattern formation: space-time plot of a network of 256 (150 are shown for clarity) mean-field coupled Stuart-Landau oscillators at $\epsilon = 16$ and $\omega = 3$. The other parameters are $Q = 0.5$ and $\Delta = 1$.

striking resemblance to the frozen random pattern solution of a coupled map lattice system [22].

V. CONCLUSION

We have explored the phenomena of AD and OD and their transitions in the paradigmatic Stuart-Landau oscillators under mean-field diffusive coupling. Using detailed eigenvalue analyses supported by bifurcation analyses, we have shown that the mean-field diffusive coupling can induce OD and also a transition between AD and OD even in identical Stuart-Landau oscillators. It has been shown that while the presence of a mean-field density parameter is not essential for inducing OD, the AD-OD transition is absolutely governed by the mean-field density parameter; the relevance of this parameter was discussed earlier in the context of genetic oscillators interacting through a quorum-sensing mechanism [20]. We have identified a dynamical state that is created by subcritical pitchfork bifurcation, namely, nontrivial AD, which coexists with the OD region. Unlike (conventional) AD, this state is destroyed by the presence of parameter mismatch. Further, in the NTAD state the occurrence of one of the two states is determined by the initial conditions. However, the observation of NTAD is subtle in natural and experimental systems as parameter mismatch is inevitable in practical coupled oscillators [23]. We have also extended our findings to a network of identical mean-field coupled Stuart-Landau oscillators where it has been shown that the AD to OD transition scenario is preserved; in this case we have shown that the coupled oscillators form a two-cluster state, the population of which depends upon the initial conditions. This study can be extended to other limit cycle and chaotic oscillators and we believe that this will improve our understanding of various mean-field coupled biological and engineering systems.

[1] A. Koseska, E. Volkov, and J. Kurths, Phys. Rep. **531**, 173 (2013).

[2] G. Saxena, A. Prasad, and R. Ramaswamy, Phys. Rep. **521**, 205 (2012).

[3] D. V. R. Reddy, A. Sen, and G. L. Johnston, Phys. Rev. Lett. **80**, 5109 (1998); **85**, 3381 (2000); A. Prasad, Phys. Rev. E **72**, 056204 (2005).

[4] P. Kumar, A. Prasad, and R. Ghosh, J. Phys. B **41**, 135402 (2008).

[5] G. B. Ermentrout and N. Kopell, SIAM J. Appl. Math. **50**, 125 (1990).

[6] A. Koseska, E. Volkov, and J. Kurths, Eur. Phys. Lett. **85**, 28002 (2009); Chaos **20**, 023132 (2010).

[7] A. Koseska, E. Ullner, E. Volkov, J. Kurths, and J. Garcá-Ojalvo, J. Theor. Biol. **263**, 189 (2010).

[8] B. F. Kuntsevich and A. N. Pisarchik, Phys. Rev. E **64**, 046221 (2001).

[9] A. Koseska, E. Volkov, and J. Kurths, Phys. Rev. Lett. **111**, 024103 (2013).

[10] W. Zou, D. V. Senthilkumar, A. Koseska, and J. Kurths, Phys. Rev. E **88**, 050901(R) (2013).

[11] A. Turing, Philos. Trans. R. Soc. London **237**, 37 (1952).

[12] K. Konishi, Phys. Rev. E **68**, 067202 (2003).

[13] R. Karnatak, R. Ramaswamy, and A. Prasad, Phys. Rev. E **76**, 035201(R) (2007).

[14] C. R. Hens, O. I. Olusola, P. Pal, and S. K. Dana, Phys. Rev. E **88**, 034902 (2013); C. R. Hens, P. Pal, S. K. Bhowmick, P. K. Roy, A. Sen, and S. K. Dana, *ibid.* **89**, 032901 (2014).

[15] M. Shiino and M. Frankowicz, Phys. Lett. A **136**, 103 (1989); R. E. Mirollo and S. H. Strogatz, J. Stat. Phys. **60**, 245 (1990); S. De Monte, F. d'Ovidio, and E. Mosekilde, Phys. Rev. Lett. **90**, 054102 (2003).

[16] A. Sharma and M. D. Shrimali, Phys. Rev. E **85**, 057204 (2012).

[17] T. Banerjee and D. Biswas, Chaos **23**, 043101 (2013).

[18] R. K. Pathria and P. D. Beale, *Statistical Mechanics*, 3rd ed. (Butterworth Heinemann, Oxford, 2011).

[19] A. Koseska, E. Volkov, A. Zaikin, and J. Kurths, Phys. Rev. E **75**, 031916 (2007).

[20] J. García-Ojalvo, M. B. Elowitz, and S. H. Strogatz, Proc. Natl. Acad. Sci. USA **101**, 10955 (2004); E. Ullner, A. Zaikin, E. I. Volkov, and J. García-Ojalvo, Phys. Rev. Lett. **99**, 148103 (2007); E. Ullner, A. Koseska, J. Kurths, E. Volkov, H. Kantz, and J. García-Ojalvo, Phys. Rev. E **78**, 031904 (2008).

[21] B. Ermentrout, *Simulating, Analyzing, and Animating Dynamical Systems: A Guide to Xppaut for Researchers and Students (Software, Environments, Tools)* (SIAM, Philadelphia, 2002).

[22] K. Kaneko, *Theory and Applications of Coupled Map Lattices (Nonlinear Science: Theory and Applications)* (Wiley, West Sussex, 1993); T. Banerjee, B. Paul, and B. C. Sarkar, Chaos **24**, 013116 (2014).

[23] T. Banerjee and D. Ghosh, arXiv:1404.0693.